

Supporting Information

Detection and Quantification of Silver Nanoparticles at Environmentally Relevant Concentrations Using Asymmetric Flow Field–Flow Fractionation Online with Single Particle Inductively Coupled Plasma Mass Spectrometry

KHANH AN HUYNH,[†] EMILY SISKA,[‡] EDWARD HEITHMAR,[§] SOHEYL TADJIKI,[¶] AND SPIROS A. PERGANTIS[#]

[†]National Research Council Post-Doctoral Associate at U.S. Environmental Protection Agency National Exposure Research Laboratory, Exposure Methods & Measurement Division
Environmental Chemistry Branch, 944 E. Harmon Avenue, Las Vegas, Nevada 89119

[‡]Chemistry Department, University of Nevada Las Vegas
4505 Maryland Parkway, Las Vegas, Nevada 89154

[§]U.S. Environmental Protection Agency, National Exposure Research Laboratory, Exposure Methods & Measurement Division, Environmental Chemistry Branch
944 E. Harmon Avenue, Las Vegas, Nevada 89119

[¶]Postnova Analytics Inc, Salt Lake City, Utah 84102

[#]Environmental Chemical Processes Laboratory, Department of Chemistry
University of Crete, Voutes Campus, Heraklion, 71103, Greece

(*E-mail: huynh.khanhan@epa.gov)

Contents

Additional Details on Experimental Section

Difficulties When Analyzing Silver Nanoparticles

Table S1. Characterization results of nanoparticles

Table S2. Composition of FL-70 detergent

Table S3. Summarized results of three consecutive AF4–spICPMS runs on a mixture containing 60 nm AgNPs and Ag-SiO₂ NPs

Figure S1. Nanoparticle size distributions

Figure S2. Representative AF4-spICPMS spike fractogram obtained from the analysis of (a) 40 nm AgNPs, (b) 60 nm AgNPs, (c) 80 nm AgNPs, (d) 100 nm AgNPs, and (e) Ag-SiO₂

Figure S3. (a) A particle number fractogram constructed from data shown in Figure 1a. (b) Representative calibration curve converting spICPMS spike signal to AgNP mass. (c) Representative calibration curve used to obtain ICPMS transport efficiency

Figure S4. Conventional AF4-ICPMS fractogram constructed from original AF4–spICPMS data presented in Figure 2a

Figure S5. Contour plot obtained from data shown in Figure 3b

References

1 **Additional Details on Experimental Section**

2 **Nanomaterials.** Citrate coated silver nanoparticles (AgNPs) (40, 60, 80, and 100 nm –
3 Citrate NanoXact™ Silver) and Ag-SiO₂ core-shell nanoparticles (Ag core and SiO₂ shell, Silica
4 Shelled 50 nm NanoXact™ Silver) were purchased from nanoComposix, Inc. (San Diego, CA).
5 The manufacturer stated that the AgNPs and Ag-SiO₂ nanoparticles (NPs) were suspended in 2
6 mM sodium citrate and isopropyl alcohol, respectively. Reference gold nanoparticles (AuNPs)
7 with particle size of 60 nm were purchased from the National Institute Standards and Technology
8 (Gaithersburg, MD). The AuNP suspensions were originally shipped in a 5 mL glass ampoules.
9 For experiments, a AuNP suspension was transferred from the ampoule to a 15 mL polypropylene
10 conical tube (Corning, Corning, NY). Extensive characterization of these nanomaterials were
11 conducted by the manufacturers¹ and some of the results are presented in Table S1. Size
12 distributions of AgNPs and Ag-SiO₂ NPs in the stock suspensions, which were provided by the
13 manufacturer, are presented in Figure S1. All the stock suspensions were stored in tightly capped
14 containers and kept in the dark at 4 °C. To homogenize the stock suspensions before used, the
15 AgNPs containers were shaken vigorously for *ca.* 30 s, while the AuNP suspension was sonicated
16 for 15 min in an ultrasonic cleaner (Model 5510, Branson Ultrasonics, Danbury, CT). All the
17 stock suspensions were used within less than 6 months after opening.

18 **Converting Ag Signal to Particle Size.** To convert Ag spike signal to particle size,
19 calibration cures were generally prepared using spICPMS (5 ms dwell-time) and diluted
20 suspensions of 40, 80, and 100 nm AgNPs (*ca.* 2 ng/L). These diluted suspensions were injected
21 directly into the ICPMS using a syringe pump (WPI SP100i, World Precision Instruments,
22 Sarasota, FL) and 20 mL disposal syringes (Thermo Fisher Scientific, Waltham, MA) at a flow
23 rate of 1.5 mL/min, which was also the rate of the flow entering the ICPMS from the AF4 during
24 AF4-spICPMS analyses. To minimize the effect of dissolution, the diluted AgNP suspensions
25 were prepared less than 5 min before spICPMS measurements. The sampling time for one
26 suspension was 4 min/run and triplicate runs were performed. Then, all the spikes having a signal
27 higher than the cut-off value were averaged. Since extremely diluted AgNP suspensions were
28 used, the maximum nanoparticle detection rate through spICPMS was about 5 – 6 particles/s.
29 Within one dwell-time, the detected Ag mass was therefore expected to equal the mass of a single
30 AgNP. The mass of AgNPs used for constructing calibration curves were calculated based on (i)

1 the assumption that AgNPs are spheres, (ii) their average TEM size, provided by the manufacture
2 (Table S1), and (ii) a density value of 10,500 kg/m³.

3 **Determination of ICPMS Transport Efficiency.** When a sample is analyzed by
4 spICPMS, the number of particles detected is equal to the number of particles in the sample
5 multiplied by the ICPMS transport efficiency (TE).² Therefore, TE is needed to estimate the
6 number nanoparticle concentrations in unknown samples. In this study, the TE values were
7 determined by using 60 nm AuNPs. Diluted AuNP suspensions with AuNP concentrations ranging
8 from *ca.* 1.4 × 10⁶ to 6.7 × 10⁵ particles/L were injected into the ICPMS at a flow rate of 1.5
9 mL/min with a 20 mL syringe and a syringe pump. The spICPMS dwell-time was 5 ms and the
10 sampling time was 4 min. Each suspension was analyzed three times. Within a spICPMS run,
11 spikes having signal higher than the predetermined cut-off value were counted as detected AuNPs.
12 Figure S3c shows a representative result a TE determination experiment. The number of detected
13 AuNPs was found to be linearly proportional to the number of injected AuNPs. The TE was the
14 slope of the linear regression curve and was found to be 0.495 in this specific case.

15 **Constructing Contour Plots.** To construct a contour plot, the AF4-spICPMS retention
16 time and count of each spike were first converted into hydrodynamic and mass-based diameters
17 using suitable calibration curves. Afterward, the two-column data (hydrodynamic and mass-based
18 diameters) was transformed into a matrix. The matrix row labels were hydrodynamic diameters,
19 starting at zero and ending at 303 nm, with an interval of 3 nm for each row label (total 101 rows).
20 The matrix column labels were mass-based diameters, starting at the closest diameter value
21 corresponding to the daily signal cut-off value for AF4-spICPMS (*e.g.*, 30, 35, or 40 nm) and
22 ending at 135 nm. The interval of each column label was 5 nm (total maximum of 21 columns).
23 Excel software then scanned the entire two-column data, and filled each matrix element with the
24 total number of particles satisfying the hydrodynamic and mass-based diameter constrains of that
25 matrix element (COUNTIFS function). Finally, a contour plot was created from the newly
26 obtained matrix using Origin software.

27 **Determination of t^0 and t_R .** To determine the void times (t^0) and nanoparticle retention
28 times (t_R), AF4-spICPMS spike fractograms were converted to particle number fractograms,
29 which are similar to the constructed conventional chromatograms presented in Pergantis et al.³
30 The y-axis of the particle number fractogram is the sum of the number of particles detected in 5 s
31 windows and the x-axis is the average retention time of each sum. A representative particle

1 number fractogram made from Figure 1a spike fractogram data is presented in SI Figure S3a.
2 Within the void region on the particle number fractogram (0 – 200 s), the occurrence time of the
3 highest frequency of Ag spikes was interpreted as the AF4–spICPMS void time. The particle
4 retention time are defined as the times at which the particles occur with the highest frequency
5 within the sample eluting region (200 – 1800 s).

6 **Evaluation of Hydrodynamic Diameter Accuracy.** Ag-SiO₂ NPs and 40, 60, and 80 nm
7 AgNPs were used to construct the hydrodynamic diameter – retention time calibration curve
8 (Figure 1b). Figure 3c shows a contour plot constructed using this 4-point calibration curve and
9 the original AF4–spICPMS data of a mixed suspension containing 60 nm AgNPs and Ag-SiO₂
10 NPs (Figure 3b). To evaluate the hydrodynamic diameter accuracy of a nanoparticle not included
11 in the calibration, a 2-point calibration was constructed from only 40 and 80 nm AgNPs and used
12 to calculate the hydrodynamic diameters of 60 nm AgNPs and Ag-SiO₂ NPs. Despite the use of
13 different hydrodynamic diameter – retention time calibrations, the two contour plots in Figure 3c
14 and SI Figure S5 were similar.

15

16 **Difficulties When Analyzing Silver Nanoparticles**

17 The spICPMS software used in this study only allows 30 min of continuous spICPMS
18 measurements. As a result, it was not possible to use a higher cross flow rate and a lower channel
19 flow rate to obtain better AF4 resolving power. However, this time constraint has its own
20 advantages, such as relatively short time for AF4–spICPMS analyses and nanoparticles – AF4
21 membrane interaction. AF4–spICPMS analyses longer than 30 minutes might be possible with
22 future releases of spICPMS software. With long spICPMS runs, signal drifting can possibly occur.
23 Significant drift was not observed during a day of the experiments in this study. Any drift could
24 be compensated by running a single standard of dissolved silver between AF4–spICPMS runs.

25 Sample aging or dissolution is a major concern when working with readily dissolved
26 nanomaterials, such as AgNPs as discussed in the manuscript. Therefore, reducing the duration of
27 AF4-spICPMS analyses and slowing down the dissolution of AgNPs are some options to obtain
28 better, reproducible results. Reducing duration of AF4-spICPMS analysis, while keeping the same
29 resolving power, requires changing channel and cross flow rates, channel thickness, membrane
30 material, and many more parameters. The dissolution of AgNPs could be potentially reduced by
31 storing the nanoparticle samples in tightly capped containers at 4 °C or in glove boxes without

- 1 oxygen. Adding a reasonable amount of citrate in the samples is likely a good option as the
- 2 dissolution of AgNPs was reported to be slower in the presence of citrate.⁴

Table S1. Characterization results of nanoparticles (provided by the manufacturers)

Particle Name	Diameter^a, nm	Hydrodynamic Diameter,^b nm	Ag/Au Mass Concentration, mg/L
40 nm AgNPs	39.0 ± 5.2	41.8	24
60 nm AgNPs	60.8 ± 6.6	62.5	20
80 nm AgNPs	79.0 ± 8.7	81.2	22
100 nm AgNPs	103.0 ± 11.0	106.5	22
Ag-SiO ₂ NPs	51.0 ^c	111.0	99
60 nm AuNPs	55.43 ^d	55.3 ± 8.3	51.86 ± 0.64

^a: Determined by using images from transmission electron microscopy (TEM), except for 60 nm AuNPs

^b: Determined by dynamic light scattering

^c: Silver core diameter

^d: Average diameter value obtained from atomic force microscopy, scanning electron microscopy, and TEM.

Table S2. Composition of FL-70 detergent⁵

Chemical	Percent
Water	88.8
Triethanolamine oleate	3.8
Sodium carbonate	2.7
Alcohols, C12-14-secondary, ethoxylated	1.8
Tetrasodium ethylenediaminetetraacetate	1.4
Polyethylene glycol	0.9
Sodium oleate	0.5
Sodium bicarbonate	0.1

Table S3. Summarized results of three consecutive AF4-spICPMS runs of a mixture containing 60 nm AgNPs (291 ng/L) and Ag-SiO₂ NPs (219 ng Ag/L). Detected particles having diameters larger than 80 nm were considered Ag-SiO₂ NPs.

Run number	60 nm AgNPs			Ag-SiO ₂ NPs		
	No. of detected particles	Ag-based dia., nm	Hydrodynamic dia., nm	No. of detected particles	Ag-based dia., nm	Hydrodynamic dia., nm
1	155	55.2	65.3	336	54.7	119.8
2	171	53.4	63.5	332	55.5	118.3
3	113	54.1	66.4	350	55.3	122.0

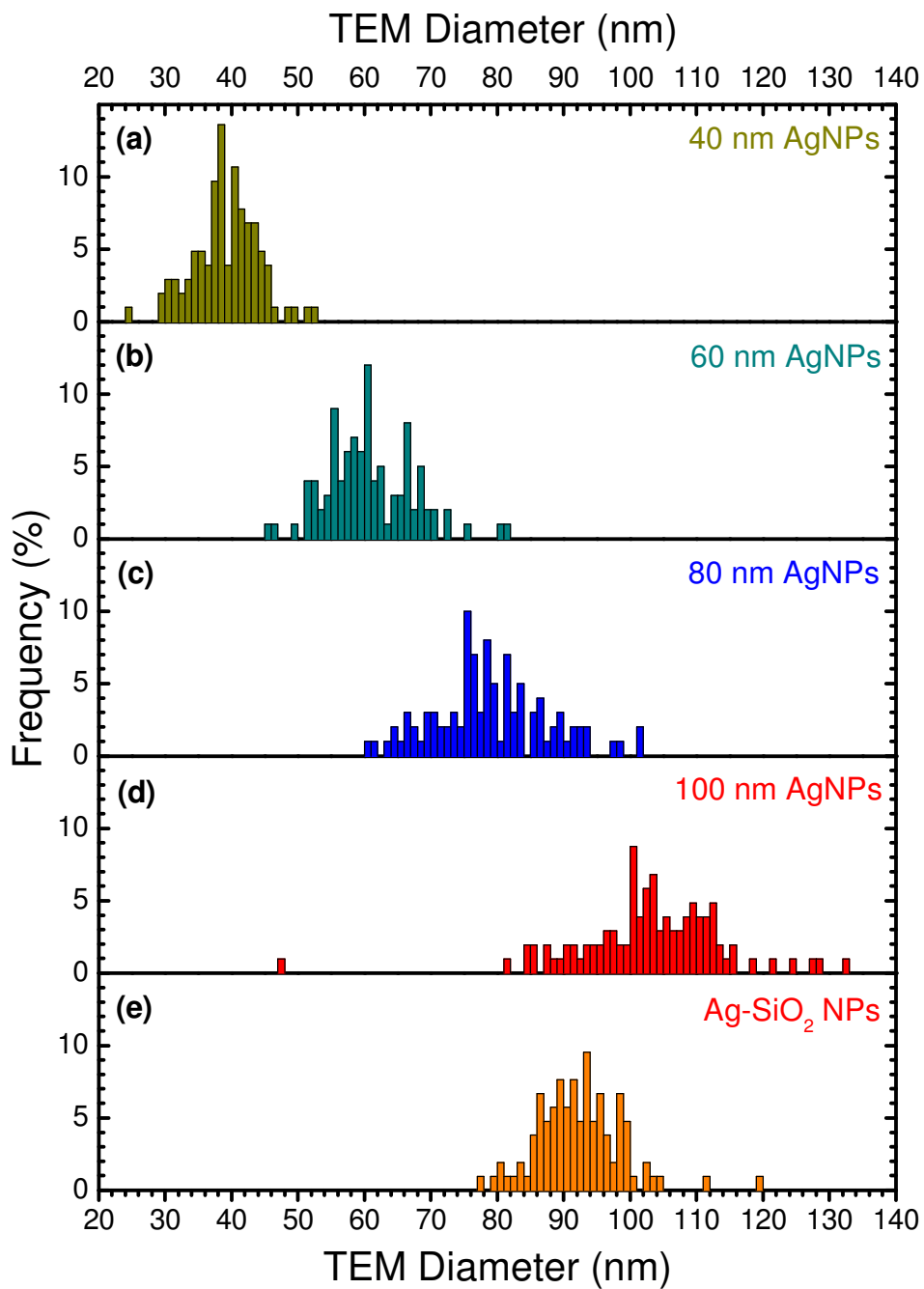


Figure S1. Nanoparticle size distributions (provided by the manufacturer – nanoComposix).

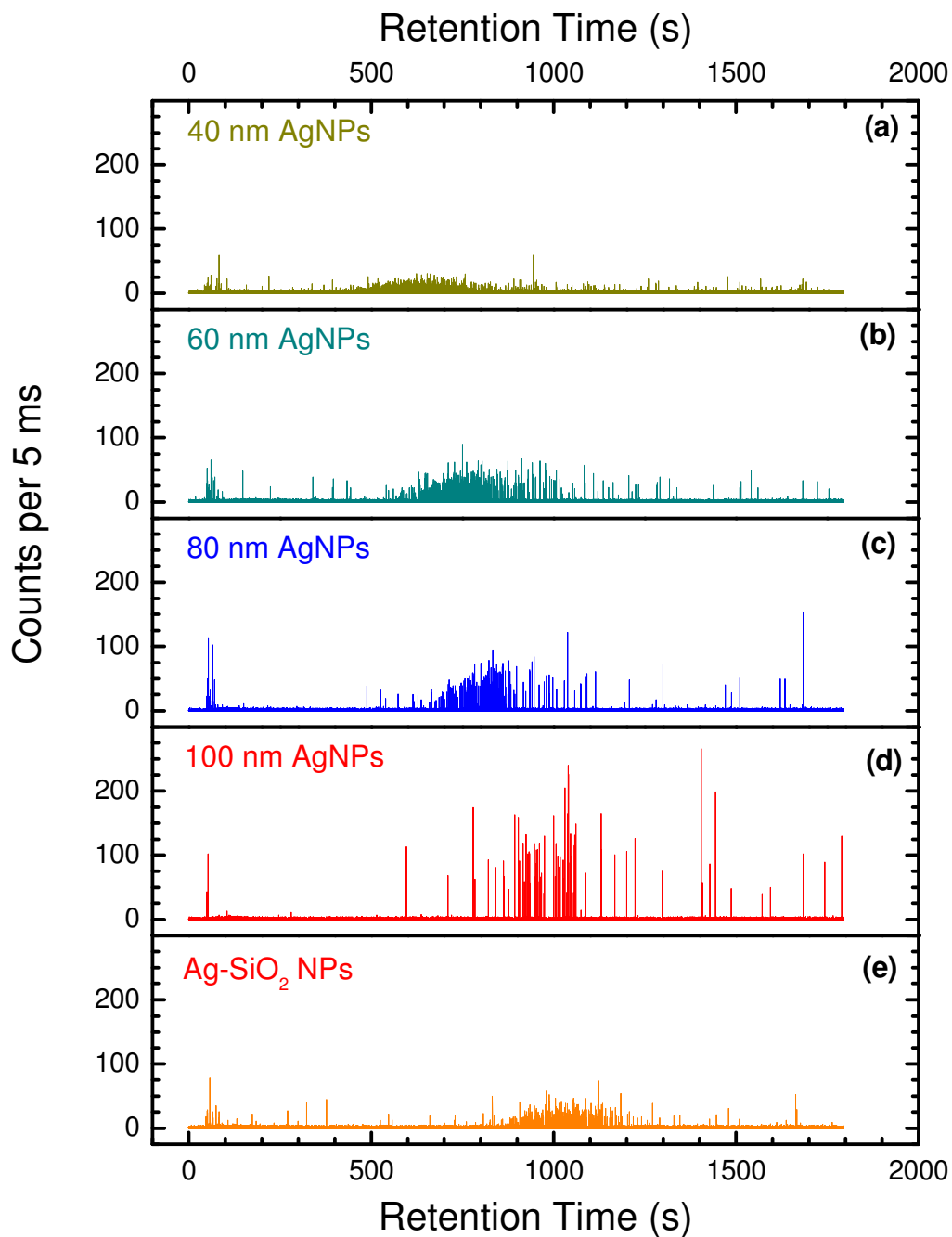


Figure S2. Representative AF4-spICPMS spike fractogram obtained from the analysis of (a) 40 nm AgNPs, (b) 60 nm AgNPs, (c) 80 nm AgNPs, (d) 100 nm AgNPs, and (e) Ag-SiO₂ NPs. The Ag-based mass concentrations of these NPs were *ca.* 500 ng/L.

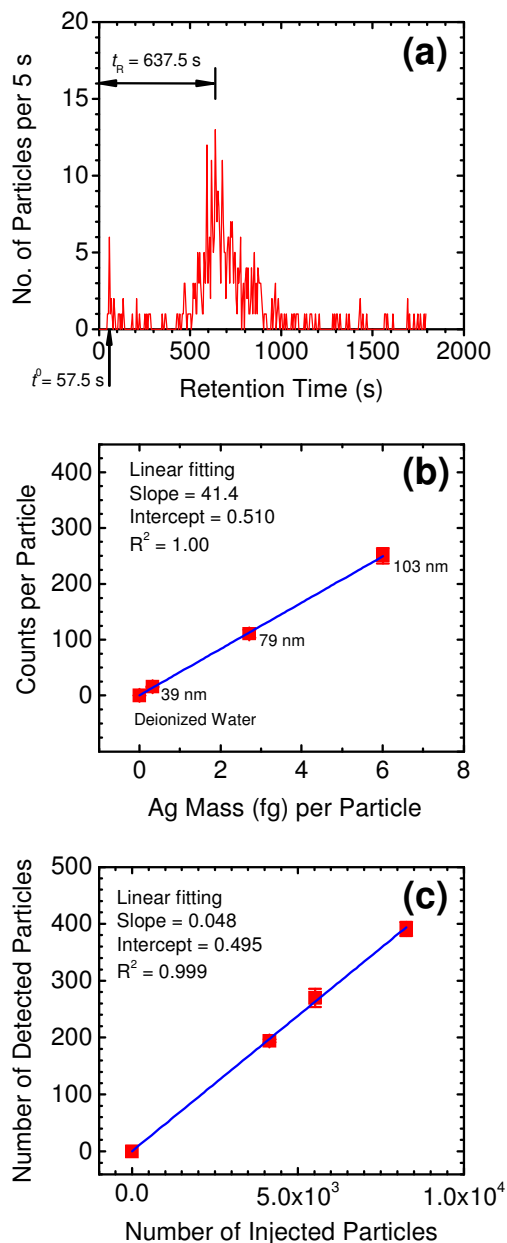


Figure S3. (a) A particle number fractogram constructed from data shown in Figure 1a. This graph is used for determining the void time (t^0) and nanoparticle retention time (t_R) from an AF4-spICPMS analysis. (b) Representative calibration curve converting spICPMS spike signal to AgNP mass. Error bars represent standard deviations of average signal obtained from three consecutive spICPMS runs (4 min/run). (c) Representative calibration curve used to obtain ICPMS transport efficiency. This experiment employed 60 nm AuNPs. Error bars represent standard deviation of number of detected AuNPs from three consecutive spICPMS runs (4 min/run).

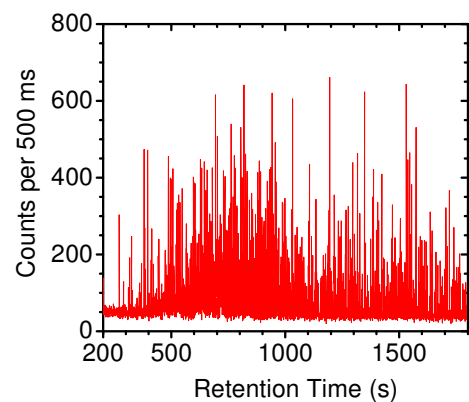


Figure S4. Conventional AF4-ICPMS fractogram constructed from original AF4–spICPMS data presented in Figure 2a. Data integration (dwell time) in this case is 500 ms, which is typical value for conventional ICPMS.

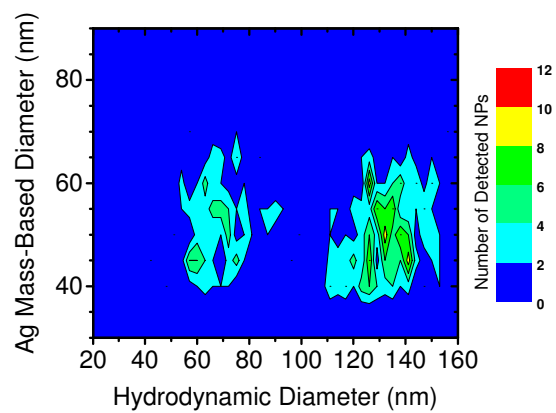


Figure S5. Contour plot obtained from data shown in Figure 3b. Only 40 nm and 80 nm AgNPs were used to construct hydrodynamic diameter – particle retention time calibration curve (slope = 5.54 and intercept = 308).

References

- (1) Report of Investigation: Reference Material 8013, Gold Nanoparticles, Nominal 60 nm Diameter; National Institute of Standards & Technology 2012.
- (2) Pace, H. E.; Rogers, N. J.; Jarolimek, C.; Coleman, V. A.; Higgins, C. P.; Ranville, J. F. *Anal Chem* **2011**, *83*, 9361-9369.
- (3) Pergantis, S. A.; Jones-Lepp, T. L.; Heithmar, E. M. *Anal Chem* **2012**, *84*, 6454-6462.
- (4) Liu, J.; Sonshine, D. A.; Shervani, S.; Hurt, R. H. *ACS nano* **2010**, *4*, 6903-6913.
- (5) pp Fisherbrand™ FL-70™ Concentrate
<https://www.fishersci.com/shop/products/fisherbrand-fl-70-concentrate-72/p-84423>.